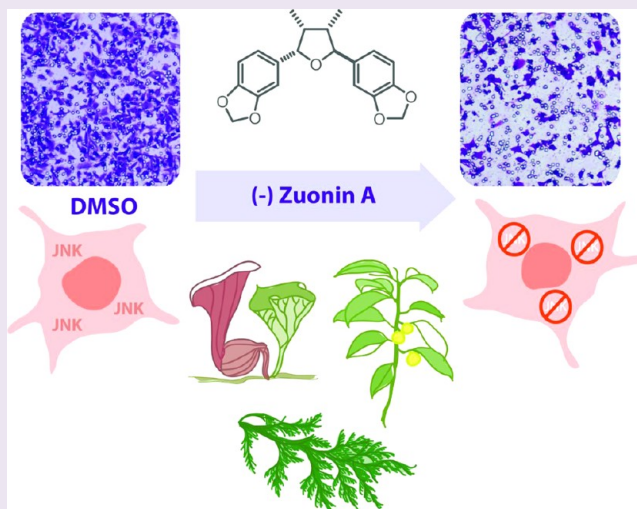


## Manipulating JNK Signaling with (–)-Zuonin A

Tamer S. Kaoud,<sup>†,‡</sup> Heekwang Park,<sup>□</sup> Shreya Mitra,<sup>#</sup> Chunli Yan,<sup>¶</sup> Chun-Chia Tseng,<sup>†</sup> Yue Shi,<sup>¶,§</sup> Jiney Jose,<sup>†</sup> Juliana M. Taliaferro,<sup>†,‡</sup> Kiyoun Lee,<sup>□</sup> Pengyu Ren,<sup>¶,§</sup> Jiyong Hong,<sup>□</sup> and Kevin N. Dalby<sup>\*,†,‡,§,||,⊥</sup><sup>†</sup>Division of Medicinal Chemistry, <sup>‡</sup>Graduate Programs in Pharmacy, <sup>§</sup>Biomedical Engineering, and <sup>||</sup>Biochemistry, <sup>⊥</sup>Texas Institute for Drug and Diagnostic Development, and <sup>¶</sup>Department of Biomedical Engineering, The University of Texas at Austin, Austin, Texas 78712, United States<sup>#</sup>The University of Texas MD Anderson Cancer Center, Houston, Texas 77030, United States<sup>□</sup>Department of Chemistry, Duke University, Durham, North Carolina 27708, United States

## S Supporting Information

**ABSTRACT:** Recently, in a virtual screening strategy to identify new compounds targeting the D-recruitment site (DRS) of the c-Jun N-terminal kinases (JNKs), we identified the natural product (–)-zuonin A. Here we report the asymmetric synthesis of (–)-zuonin A and its enantiomer (+)-zuonin A. A kinetic analysis for the inhibition of c-Jun phosphorylation by (–)-zuonin A revealed a mechanism of partial competitive inhibition. Its binding is proposed to weaken the interaction of c-Jun to JNK by approximately 5-fold, without affecting the efficiency of phosphorylation within the complex. (–)-Zuonin A inhibits the ability of both MKK4 and MKK7 to phosphorylate and activate JNK. The binding site of (–)-zuonin A is predicted by docking and molecular dynamics simulation to be located in the DRS of JNK. (+)-Zuonin A also binds JNK but barely impedes the binding of c-Jun. (–)-Zuonin A inhibits the activation of JNK, as well as the phosphorylation of c-Jun in anisomycin-treated HEK293 cells, with the inhibition of JNK activation being more pronounced. (–)-Zuonin A also inhibits events associated with constitutive JNK2 activity, including c-Jun phosphorylation, basal Akt activation, and MDA-MB-231 cell migration. Mutations in the predicted binding site for (–)-zuonin A can render it significantly more or less sensitive to inhibition than wild type JNK2, allowing for the design of potential chemical genetic experiments. These studies suggest that the biological activity reported for other lignans, such as saucerneol F and zuonin B, may be the result of their ability to impede protein–protein interactions within MAPK cascades.



In mammals, JNKs (c-Jun N-terminal kinases) are encoded by three different genes (*jnk1*, *jnk2*, and *jnk3*) that are alternatively spliced to produce a total of approximately 10 different isoforms. The predominant genes *jnk1* and *jnk2* are expressed ubiquitously, while *jnk3* is mainly expressed in neuronal tissues, the testes, and to a lesser extent in cardiac myocytes.<sup>1</sup> As a member of the mitogen-activated protein kinase (MAPK) family, JNKs regulate various cellular functions.<sup>2</sup> Hyperactivation of JNK occurs in a number of disease states, including type I and type II diabetes, Alzheimer's disease, arthritis, asthma, atherosclerosis, heart failure, and Parkinson's disease.<sup>3</sup> Cellular stressors, including cytokines, hypoxia, UV light, and osmotic stress, stimulate JNK activity, leading to pro-inflammatory, mitogenic, or apoptotic signals,<sup>4</sup> which may contribute to the oncogenic functions of JNK.<sup>5</sup>

JNK1 plays an important role in human hepatocellular carcinoma<sup>6</sup> and accelerates the development of chronic colitis-

induced colorectal cancer.<sup>7</sup> Moreover, the JNK pathway is implicated in PI3K-driven human prostate cancer, where PTEN is often found inactivated, leading to increased AKT activity and elevated JNK activation, which in turn contributes to tumor cell proliferation and angiogenesis.<sup>8</sup> However, JNK1 is also reported to act as a tumor suppressor in DMBA/TPA-induced skin tumors and in spontaneous colon cancer, highlighting the complexities of JNK signaling.<sup>9,10</sup> JNK2 is constitutively activated in glial tumor cell lines<sup>11</sup> and human glioblastoma models<sup>12</sup> and is implicated in the activation of Akt and overexpression of eukaryotic translation initiation factor 4 (eIF4E).<sup>12</sup>

Received: May 26, 2012

Accepted: August 23, 2012

Published: August 23, 2012

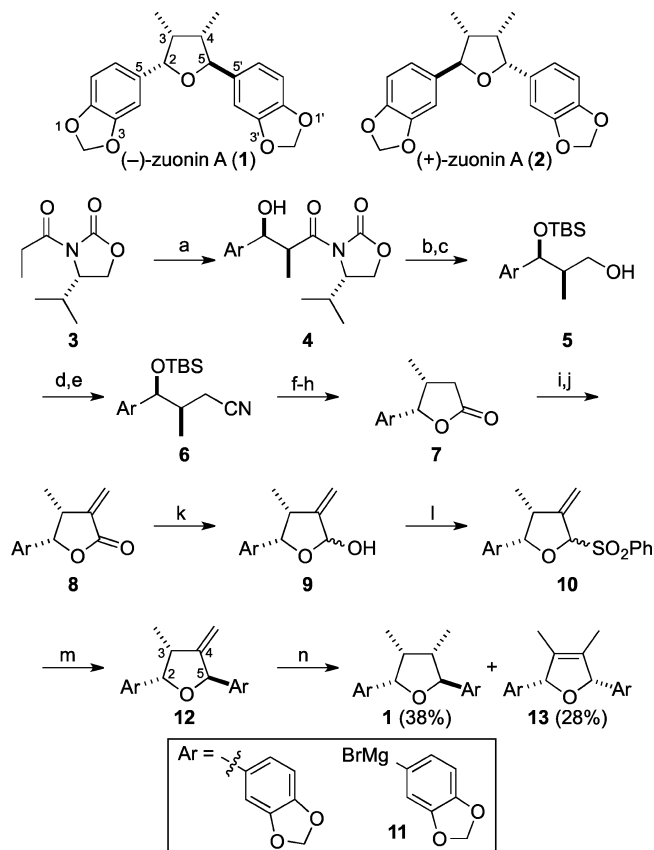
Interestingly, both JNK1 and JNK2 reportedly regulate cell migration,<sup>13</sup> and JNK2 has been shown to promote mammary cancer cell migration by specifically altering both the expression and trafficking of epidermal growth factor substrate 8 (EPS8) as well as its critical protein binding interactions, which connect growth factor signaling to the actin cytoskeleton during cell migration.<sup>14</sup> Cell migration is an essential process associated with tissue repair and regeneration, atherosclerosis, arthritis, mental retardation, embryonic morphogenesis, and cancer metastasis.<sup>15</sup> Recently we reported the design of peptide inhibitors that selectively targeted the protein-binding site of the JNK2 isoform and efficiently inhibit breast cancer cell migration.<sup>16</sup> Taken together, this reveals the importance of the JNKs as attractive targets for the treatment of a variety of diseases, especially cancer. However, no inhibitors of JNK have been approved for use in humans.<sup>17</sup>

JNKs are mainly activated by phosphorylation of the activation loop at a Thr-Pro-Tyr (TPY) motif by the MAP2Ks MKK4 and MKK7<sup>18</sup> and are deactivated by MAPK phosphatases including MKP1 and MKP5. The JNK2 isoform is uniquely autophosphorylated without the requirement of MKK4 and MKK7.<sup>19</sup> Scaffolding proteins such as JIP<sup>20</sup> and arrestin<sup>21</sup> can assemble signaling complexes consisting of a MAP3K, a MAP2K, and a MAPK to promote specific JNKs.

Unlike ATP-competitive inhibitors, non-canonical inhibitors targeting protein interaction sites of JNK may disrupt the binding of JNK to upstream and downstream proteins, including phosphatases and scaffolds, resulting in the alteration of JNK signaling in cells. An important advantage of such non-ATP competitive inhibitors is that they do not have to compete with an intracellular ligand that is present at high millimolar concentrations, such as ATP. In addition, inhibitors that target protein binding sites may be uniquely specific for JNK.<sup>22</sup> Some trials have been conducted to discover small molecules targeting the protein-binding site of JNK. In 2008, Stebbins *et al.* discovered that the thiadiazole BI-78D3 (the first small molecule targeting the JNK-JIP interaction)<sup>23</sup> efficiently displaces biotinylated pepJIP1 from GST-JNK1 with an IC<sub>50</sub> of 500 nM. Additional reports have focused on the development of BI-78D3 and the enhancement of its plasma stability,<sup>22</sup> while others still continue the search for different scaffolds or peptides that act as inhibitors of the JNK-protein interaction.<sup>22,24</sup>

The largely solvent-exposed and relatively shallow protein docking sites of JNK<sup>25</sup> make the discovery and design of potent non-canonical inhibitors targeting the protein binding sites of MAP kinases difficult. Recently, we attempted to overcome this challenge by employing computational studies. Using virtual screening, a group of inhibitors targeting the JNK-JIP binding site was discovered.<sup>26</sup> One of these inhibitors, known as (-)-zuonin A (1, Scheme 1), selectively inhibits JNK over ERK2 and p38 MAPK. (-)-Zuonin A (1) is a 2,5-diaryl-3,4-dimethyltetrahydrofuranoid lignan which has been isolated from *Aristolochia chilensis*,<sup>27</sup> *Saururus cernuus*,<sup>28</sup> *Piper schmidtii*,<sup>29</sup> *Chamaecyparis obtusa var. formosana*,<sup>30</sup> and *Piper futokadsura*.<sup>31</sup> Notably, two recent reports have implicated other lignan derivatives as having biological effects resulting from their activity toward MAP kinases. For example, saucerneol F, a tetrahydrofuran-type sesquigignan isolated from *Saururus chinensis*, inhibits nitric oxide (NO) production in a dose-dependent manner. This effect is accompanied by reduction of the inducible nitric oxide synthase (iNOS) protein and mRNA expression in lipopolysaccharide (LPS)-stimulated

### Scheme 1. Asymmetric Synthesis of (-)-Zuonin A<sup>a</sup>



<sup>a</sup>Reagents and conditions: (a) *n*-Bu<sub>2</sub>BOTf, Et<sub>3</sub>N, CH<sub>2</sub>Cl<sub>2</sub>, -78 °C, 30 min, then piperonal, -78 °C, 1 h, 78%; (b) TBSCl, imidazole, DMF, 25 °C, 14 h, 90%; (c) LiBH<sub>4</sub>, MeOH, Et<sub>2</sub>O, 0 °C, 1 h, 79%; (d) MsCl, Et<sub>3</sub>N, CH<sub>2</sub>Cl<sub>2</sub>, -78 °C, 30 min; (e) NaCN, DMSO, 70 °C, 2 h, 97% for 2 steps; (f) TBAF, THF, 25 °C, 1 h; (g) NaOH, THF/MeOH/H<sub>2</sub>O (1:1:1), reflux, 16 h; (h) PPTS, toluene, 80 °C, 2 h, 91% for 3 steps; (i) LiHMDS, THF, -78 °C, 30 min, then Eschenmoser's salt, -78 °C, 15 min; (j) *m*-CPBA, NaHCO<sub>3</sub>, THF, 25 °C, 30 min, 95% for 2 steps; (k) DIBALH, CH<sub>2</sub>Cl<sub>2</sub>, -78 °C, 10 min, 87%; (l) PhSO<sub>2</sub>H, CaCl<sub>2</sub>, CH<sub>2</sub>Cl<sub>2</sub>, 25 °C, 10 min, 66%; (m) 11, ZnBr<sub>2</sub>, THF, 25 °C, 30 min, 76%; (n) Pd/C, H<sub>2</sub>, EtOAc/MeOH (3:1), 25 °C, 1 h, 38%, dr = 5:1.

murine macrophage (RAW264.7) cells. Saucerneol F was reported to attenuate NO production and iNOS expression by blocking LPS-induced activation of NF-κB (NF-kappaB), AP-1, and most MAP kinases (including ERK1/2, p38 MAPK, and JNK).<sup>32</sup> Zuonin B, a stereoisomer of zuonin A, isolated from the flower buds of *Daphne genkwa*, is reported to exhibit immunological effects in RAW264.7 cells due to its ability to suppress the levels of nitric oxide, prostaglandin E<sub>2</sub>, and pro-inflammatory cytokines such as tumor necrosis factor-α and interleukin-6. The detailed study of its molecular mechanism demonstrated its ability to reduce NF-κB activation by suppressing proteolysis of IκBα and p65 nuclear translocation, as well as by inhibiting the phosphorylation of ERK 1/2 and JNK.<sup>33</sup> On the basis of these data saucerneol F and zuonin B have been proposed to be anti-inflammatory agents. It remains to be established whether they directly bind and inhibit MAPKs.

Here we describe the asymmetric synthesis of the lignans (-)-zuonin A and (+)-zuonin A and report both biochemical and biological approaches employed to show that (-)-zuonin A

is an inhibitor of JNK. We identified two mechanisms as likely contributors to its ability to inhibit JNK signaling in cells.

## RESULTS AND DISCUSSION

**Synthesis of (–)-Zuonin A and (+)-Zuonin A.** Recently, (–)-zuonin A (**1**, Scheme 1) was identified as an inhibitor of JNK following a virtual screening analysis designed to identify small molecule inhibitors of JNK-protein interactions.<sup>26</sup> While there are several reports of its isolation and structure determination in the literature,<sup>27–31</sup> its synthesis has not been reported. In addition, the absolute configuration of (–)-zuonin A (**1**) has not been established. Therefore, as part of an ongoing effort to characterize bioactive lignans we embarked on the total synthesis of (–)-zuonin A (**1**), drawing on our recent synthesis of substituted tetrahydrofurans.<sup>34,35</sup> To this end we report a synthetic route that affords (–)-zuonin A (**1**) and its enantiomer (+)-zuonin A (**2**). As a result, the absolute configuration of (–)-zuonin A (**1**) and (+)-zuonin A (**2**) is now assigned.

**Synthesis of Intermediate 7.** The first stages of the synthesis involve the preparation of the chiral dihydrofuranone **7** (Scheme 1), which was accomplished following previously reported procedures.<sup>34</sup> Thus, commercially available (4*S*)-4-(1-methylethyl)-3-(1-oxopropyl)-2-oxazolidinone **3** was reacted with piperonal in the presence of *n*-Bu<sub>2</sub>BOTf and Et<sub>3</sub>N to provide the desired *syn*-adol adduct **4** in 78% yield as a single diastereomer.<sup>36</sup> Protection of **4** with TBSCl (90%) followed by LiBH<sub>4</sub> reduction (79%) provided the corresponding alcohol **5**. Protection of **5** with MsCl and subsequent treatment with NaCN accomplished one-carbon homologation to give **6** (97% for two steps). TBS deprotection by TBAF, hydrolysis of the nitrile group to the corresponding carboxylic acid, and acid-catalyzed lactonization provided **7** in 91% for three steps.

**Elaboration of 1 from 7.** As demonstrated in the stereoselective synthesis of manassantins A and B, we envisioned that the installation of a sterically less demanding *exo*-methylene group as a precursor to the C4 methyl group would direct the addition of **11** via the “inside attack” model to provide the desired 2,3-*cis*-2,5-*trans*-tetrahydrofuran **12**.<sup>35</sup> Alkylation of **7** with Eschenmoser’s salt and *m*-CPBA oxidation smoothly proceeded to afford **8** in 95% for two steps.<sup>37,38</sup> Reduction of **8** with DIBALH followed by treatment with PhSO<sub>2</sub>H provided 2-benzenesulfonyl cyclic ether **10**. As expected, the *exo*-methylene group in **10** directed the addition of **11** to provide the desired 2,3-*cis*-2,5-*trans*-tetrahydrofuran **12** as a single diastereomer (76%). As demonstrated in the synthesis of manassantins A and B,<sup>35</sup> catalytic hydrogenation under conventional conditions (H<sub>2</sub>, Pd/C, EtOAc/MeOH) completed the asymmetric synthesis of **1** (38%, dr = 5:1, 97.7% ee). It should be noted that the double bond isomerization occurred during the catalytic hydrogenation reaction to give **13** (28%).

The optical rotation of **1** obtained by synthesis enabled the assignment of absolute configuration of **1**. The enantiomer (+)-zuonin A (**2**) was also prepared in a similar manner starting from the enantiomer of **3**, (4*R*)-4-(1-methylethyl)-3-(1-oxopropyl)-2-oxazolidinone.

**In Vitro Studies on the Mechanism of (–)-Zuonin A Identifies a Mechanism of Partial Competitive Inhibition.** (–)-Zuonin A Inhibits *c*-Jun Phosphorylation by JNK. (–)-Zuonin A was initially discovered as an inhibitor of JNK through *in silico* screening.<sup>26</sup> We hypothesized that small molecules that bind the D-recruitment site (DRS) of JNK, a

recruitment site utilized by substrates and other protein scaffolds to dock onto and recognize MAPKs,<sup>39</sup> would block the ability of JNK to efficiently engage protein ligands. To characterize the enantiomers of zuonin A, we first tested their ability to inhibit the phosphorylation of GST-*c*-Jun (2 μM) by activated JNK1, JNK2, and JNK3. As several kinetic studies of the JNKs have been reported,<sup>40</sup> we used these to guide the design of our kinetic investigations. First, we obtained dose–response curves for each enantiomer. (–)-Zuonin A exhibits IC<sub>50</sub> values in the range of 1.7–2.9 μM, plateauing at around 75% of the theoretical maximal level of inhibition when (–)-zuonin A is saturating (Table 1 and Figure 1a). In contrast,

**Table 1. Selectivity of (–)-Zuonin A**

kinase	IC <sub>50</sub> (μM) <sup>a</sup>	% inhibition at saturating (–)-zuonin A (200 μM)
JNK1	1.7 ± 0.26	75
JNK2	2.9 ± 0.17	70
JNK3	1.74 ± 0.16	73
WT-MKK4 <sup>a</sup>	1.8 ± 0.17	77
WT-MKK7 <sup>a</sup>	1.99 ± 0.15	50
ERK1	>200	10
ERK2	>200	10
p38MAPKα	>200	20
p38MAPKβ	no inhibition	15
p38MAPKγ	>200	10
p38MAPKδ	>200	10

<sup>a</sup>Inhibits the phosphorylation of JNK.

while exhibiting similar IC<sub>50</sub> values, the level of inhibition achieved by saturating (+)-zuonin A is only 8–14% of the theoretical maximum (Figure 1b). To understand these observations further we determined the observed rate constant, *k*<sub>obs</sub>, over a range of *c*-Jun concentrations at different fixed concentrations of (–)-zuonin A, in the presence of a saturating concentration of MgATP. The double reciprocal plot derived from this study (Figure 2a) is consistent with a mechanism of partial-competitive inhibition (Figure 2b, where α ≈ 5, β = 1, and *K*<sub>i</sub> ≈ 2.7 ± 0.4 μM). According to this model, (–)-zuonin A binds JNK and weakens its affinity for *c*-Jun by approximately 5-fold (α ≈ 5) without affecting *k*<sub>cat</sub> (β = 1). It is reasonable to propose that (+)-zuonin A follows a similar mechanism but only marginally weakens the affinity of JNK for *c*-Jun (α ≈ 1), presumably because it adopts a binding mode that does not impede the recognition of *c*-Jun by the DRS.

**(–)-Zuonin Inhibits the Activation of JNK1 by MKK4 and MKK7.** JNK is activated by the dual-specificity kinases MKK4 and MKK7, which preferentially phosphorylate on Tyr-185 and Thr-183, respectively.<sup>18</sup> These kinases are reported to bind JNK within the DRS in a similar manner to the JIP scaffold and *c*-Jun protein substrate.<sup>41</sup> Thus, (–)-zuonin A is predicted to impede the binding of MKK4 and MKK7 to the inactive form of JNK. Indeed, we discovered that (–)-zuonin A does inhibit the phosphorylation of JNK1 by both kinases. Figure 3a shows a dose–response curve for the phosphorylation of JNK1 by MKK4 or MKK7 where the concentration of (–)-zuonin A was varied from 0 to 200 μM. These reveal values of IC<sub>50</sub> similar to those obtained with the active JNKs, and furthermore a submaximal level of inhibition is observed at saturating (–)-zuonin A, suggestive again of a partial-competitive inhibition mechanism.

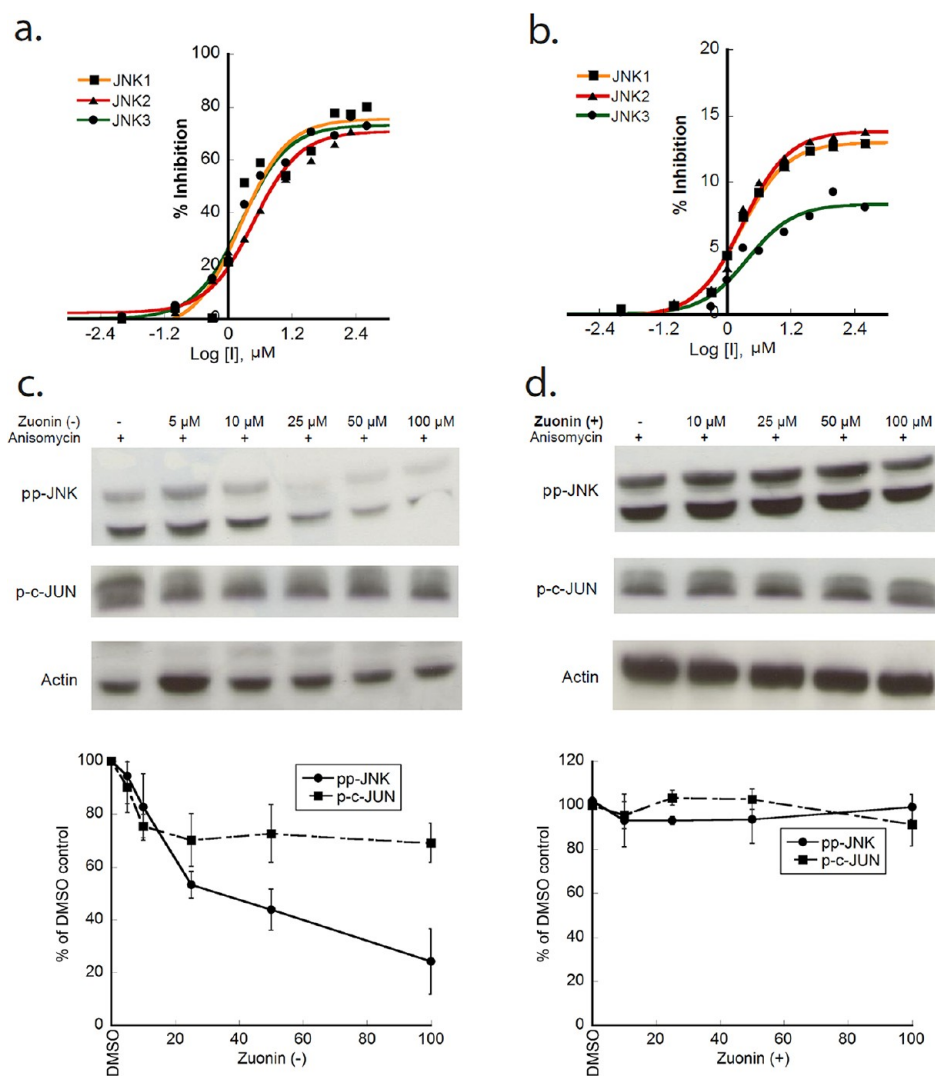


**Figure 1.** (–)-Zuonin A, but not (+)-zuonin A, is a potent JNK inhibitor in *in vitro* cell-free and cell-based kinase assays. (a) The effect of (–)-zuonin A on the ability of JNK1, JNK2 and JNK3 to phosphorylate GST-c-Jun (1–221). Data were fitted to eq 4. (b) The effect of (+)-zuonin A on the ability of JNK1, JNK2, and JNK3 to phosphorylate GST-c-Jun (1–221). Data were fitted to eq 4. (c) HEK293 cells were treated with a DMSO control or (–)-zuonin A (5–100  $\mu\text{M}$ ) for 12 h. The JNK pathway was then induced by the addition of anisomycin (50–100 nM) for 5–10 min before lysing the cells. Lysates were fractionated by SDS-PAGE (10% gel) and subjected to Western blot analysis in order to detect the phosphorylated forms of c-Jun and JNK. A graphical analysis is shown, representative of three independent experiments. (d) As in panel c using (+)-zuonin A.

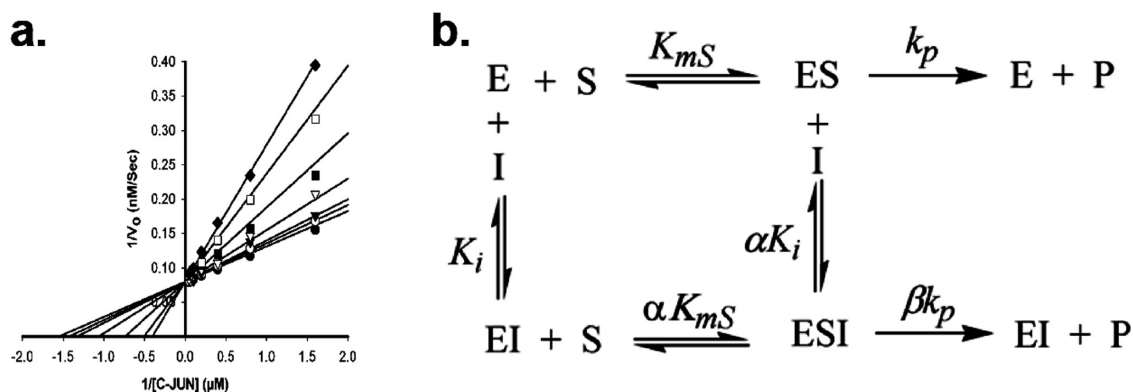


**Figure 2.** Mechanism of JNK inhibition by (–)-zuonin A. (a) Double reciprocal plot of  $1/V_0$  vs  $1/[\text{c-Jun}]$  at varied fixed concentrations of (–)-zuonin A (0–50  $\mu\text{M}$ ) and 0.5 mM MgATP. Initial velocities were measured using various (0.63–20  $\mu\text{M}$ ) concentrations of c-Jun. The data were fitted to a model of partial competitive inhibition according to eq 3, where  $k_{\text{cat}}^{\text{app}} = 1.2 \pm 0.08 \text{ s}^{-1}$ ,  $K_m^{\text{app}} = 1.6 \pm 0.03 \mu\text{M}$ ,  $K_i^{\text{app}} = 2.7 \pm 0.4 \mu\text{M}$ ,  $\alpha K_m^{\text{app}} = 8 \pm 0.2$ ,  $\alpha = 5 \pm 0.3$ , and  $\beta = 1$ . (b) Proposed mechanisms of partial competitive C-Jun inhibition by (–)-zuonin A.

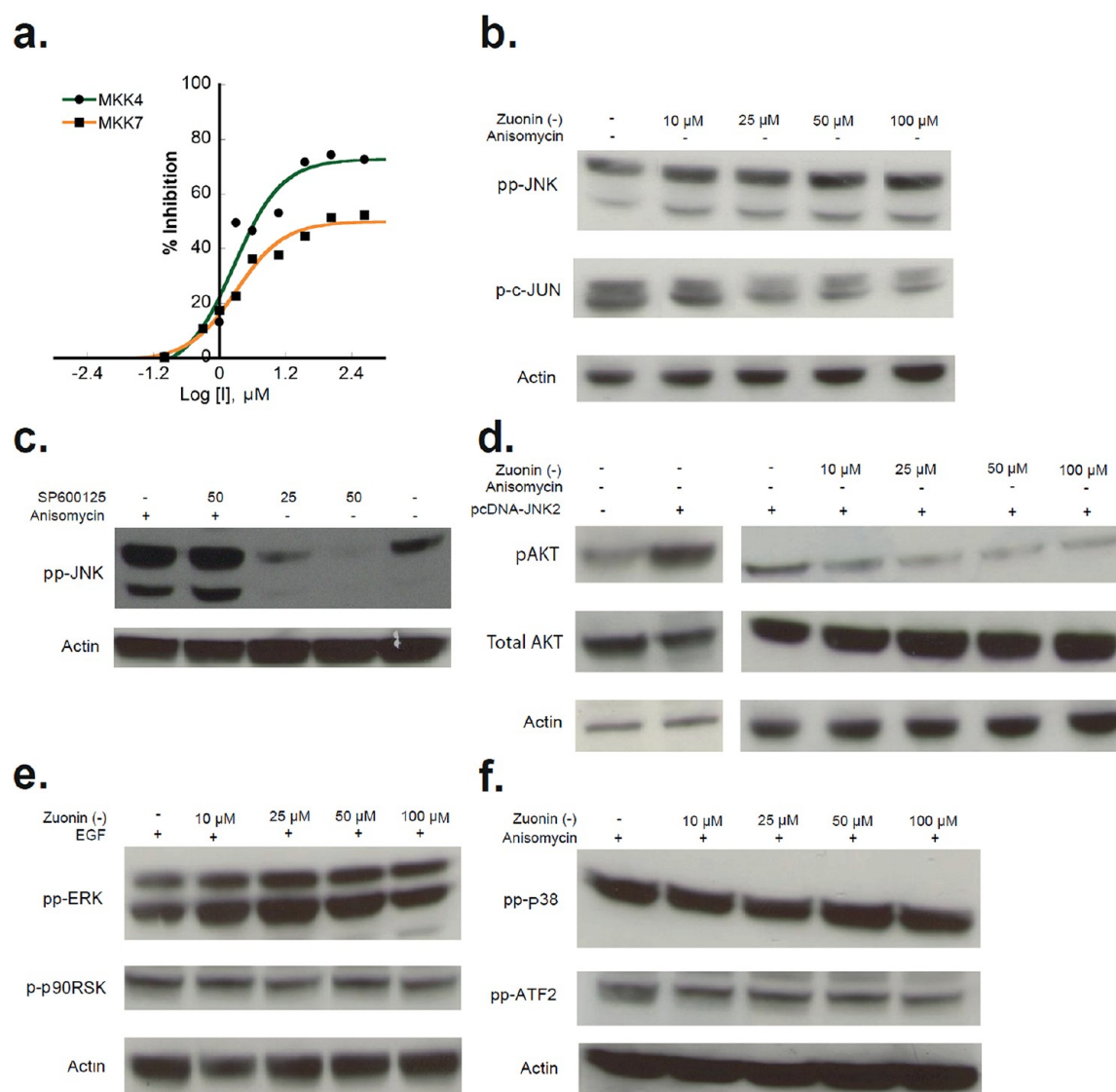


**Figure 3.** Mechanism of JNK inhibition by (–)-zuonin A in HEK293T cells. (a) The effect of (–)-zuonin A on the ability of active MKK7 (WT) and active MKK4 (WT) to phosphorylate inactive JNK1 with  $IC_{50} \approx 2.0 \pm 0.15$  and  $1.8 \pm 0.17 \mu\text{M}$ , respectively. Data were fitted to eq 4. (b) HEK293T cells were transfected with WT-JNK2 and treated with a DMSO control or different concentrations of (–)-zuonin A without induction by anisomycin. A graphical analysis is shown in Figure 4d. (c) HEK293T cells were transfected with WT-JNK2 and treated with a DMSO control or two concentrations of SP600125 (ATP-competitive JNK inhibitor) with and without induction by anisomycin. (d) HEK293T cells were transfected either with empty pcDNA3 vector or with WT-JNK2 and treated with a DMSO control or different concentrations of (–)-zuonin A without induction by anisomycin. (–)-Zuonin A did not inhibit AKT expression but inhibited AKT phosphorylation. (e) Specificity of (–)-zuonin A toward ERK2 in HEK293 cells. Cells were treated with a DMSO control or with (–)-zuonin A (0–100  $\mu\text{M}$ ) for 12 h. The ERK2 pathway was then induced by 50 ng of EGF (Epidermal Growth Factor) for 5–10 min before lysing the cells. Lysates were fractionated by SDS-PAGE (10% gel) and subjected to Western blot analysis in order to detect the phosphorylated forms of ERK and p90RSK (p90 Ribosomal S6 Kinase). (f) Specificity of (–)-zuonin A toward p38 MAPKs in HEK293 cells. Cells were treated with a DMSO control or (–)-zuonin A (10–100  $\mu\text{M}$ ) for 12 h. The p38 pathway was induced by the addition of anisomycin (50–100 nM) for 5–10 min before lysing the cells. Lysates were fractionated by SDS-PAGE (10% gel) and subjected to Western blot analysis in order to detect the phosphorylated forms of p38 and ATF2.

**Cellular Studies. Inhibition of JNK Activation.** The effect of both enantiomers of zuonin A on the activation of JNK or on the phosphorylation of c-Jun following cell stimulation by anisomycin (which activates the JNK pathway) was assessed in HEK293 cells by Western blot analysis. Assessment of the phosphorylation of c-Jun, an *in vivo* substrate of the JNKs,<sup>42</sup> as determined using an antiphospho-Ser-63 antibody, shows it is clearly blunted by the addition of (–)-zuonin A, but not by a DMSO control (Figure 1c). Anisomycin has been reported to induce the appearance of two bands of phosphorylated c-Jun.<sup>43</sup> Migration from the lower band to the upper band has been

suggested to be due to phosphorylation of Thr-91 and/or Thr-93, in addition to Ser-63 and Ser-73.<sup>43</sup> Interestingly, Figure 1c also shows that (–)-zuonin A blunts the activation of the JNK isoforms in cells in a dose-dependent manner. It should be noted that the phospho JNK antibody used in this study does not distinguish between the JNK isoforms. (–)-Zuonin A inhibits JNK activation to a greater extent than it inhibits c-Jun phosphorylation, reflecting the likelihood that complete c-Jun phosphorylation is achieved upon activation of only a fraction of cellular JNK. Figure 1d shows that (+)-zuonin A inhibits neither JNK activation nor c-Jun phosphorylation, consistent

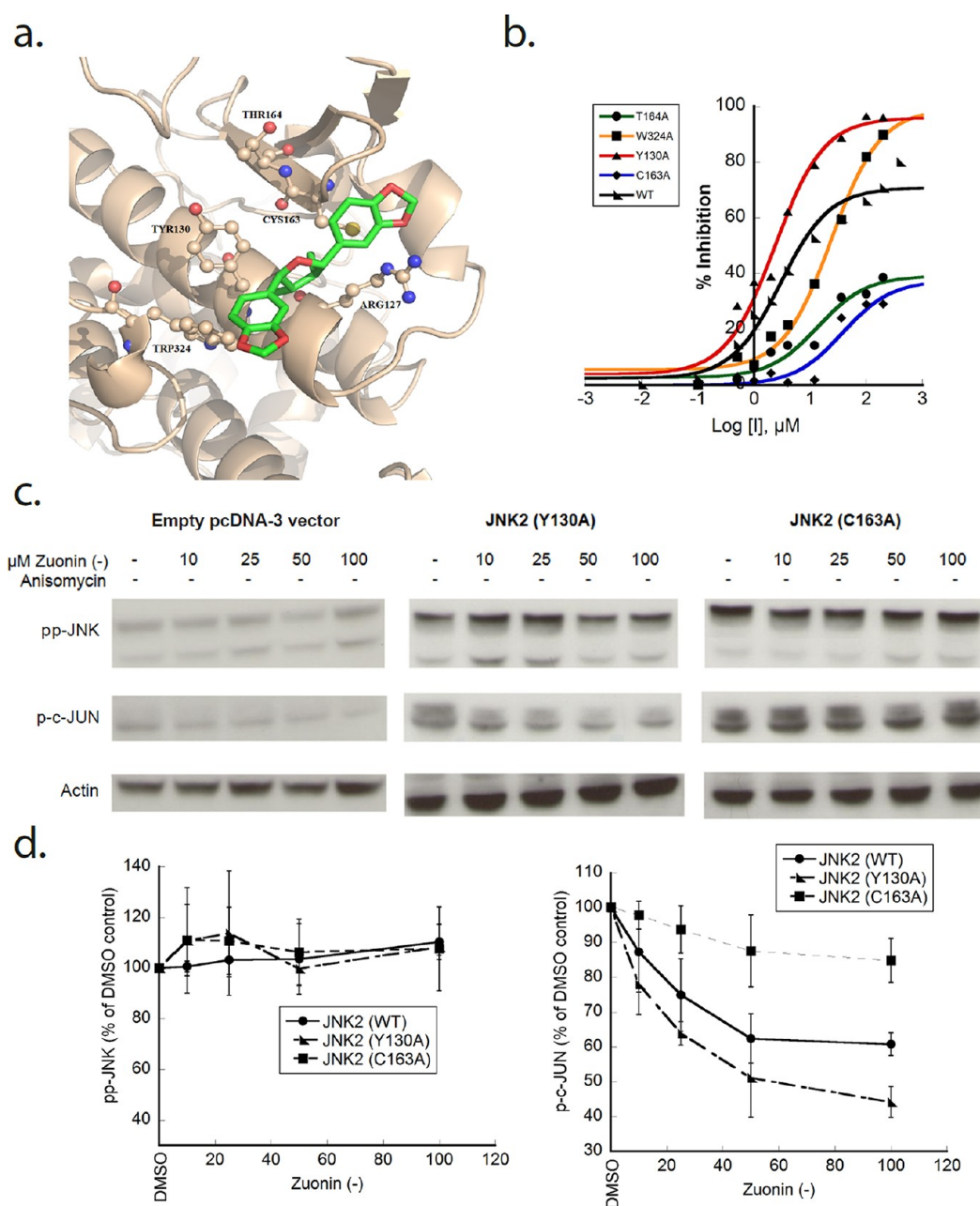


**Figure 4.** Altering JNK sensitivity to (-)-zuonin A. (a) MD trajectories for (-)-zuonin A binding to JNK1 (PDB ID: 1UKH).<sup>51</sup> The figure was generated using PyMol software (<http://pymol.sourceforge.net/>). (b) The effect of different JNK2 DRS site mutations on the sensitivity of JNK2 toward (-)-zuonin A, detected by measuring the ability of each mutant to phosphorylate GST-c-Jun (1–221) in the presence of (-)-zuonin A. Data were fitted to eq 4. (c) HEK293 cells were transfected with empty pcDNA 3 vector, JNK2 (Y130A), or JNK2 (C163A) and treated with different concentrations of (-)-zuonin A (0–100  $\mu\text{M}$ ). Subsequent phosphorylation of JNK and c-Jun was detected by Western blot. (d) Graphical analysis for the effect of different JNK2 DRS site mutations on the sensitivity of JNK2 toward (-)-zuonin A in HEK293T cells, representative of three independent experiments. Lysates were fractionated by SDS-PAGE (10% gel) and subjected to Western blot analysis in order to detect the phosphorylated forms of c-Jun and JNK.

with its decreased ability to inhibit the JNKs in the kinase assays (Figure 1a and b).

**Investigating JNK Self-Activation. (-)-Zuonin A Does Not Inhibit JNK2 Autoactivation.** The JNK2 isoforms exhibit an ability to self-phosphorylate on the same residues phosphorylated by MKK4 and MKK7 both *in vitro* and in cells, leading to their activation.<sup>19</sup> Figure 3b shows that when overexpressed in HEK293T cells JNK2 $\alpha$ 2 becomes phosphorylated. As it is not known whether the DRS of JNK2 $\alpha$ 2 is important for autophosphorylation, we incubated cells with (-)-zuonin A

and assessed the phosphorylation status of the overexpressed JNK2 $\alpha$ 2 by Western blot analysis. We found that (-)-zuonin A is unable to inhibit JNK2 $\alpha$ 2 autophosphorylation even at a concentration of 100  $\mu\text{M}$ . In contrast, the phosphorylation of c-Jun, which is mediated by the overexpressed JNK2 $\alpha$ 2, is clearly blunted upon treatment of the cells with (-)-zuonin A with an ED<sub>50</sub> of approximately 25  $\mu\text{M}$  (Figure 3b). This provides strong evidence that (-)-zuonin A binds JNK2 $\alpha$ 2 in cells and impedes the interaction between JNK2 $\alpha$ 2 and c-Jun but does not prevent constitutive JNK2 $\alpha$ 2 phosphorylation resulting from

Table 2. Effect of JNK2 Mutations on the Sensitivity of JNK towards (–)-Zuonin A

mutants	$K_m^b$ ( $\mu\text{M}$ )	$k_{\text{cat}}^b$ ( $\text{s}^{-1}$ )	$k_{\text{cat}}/K_m$ ( $\mu\text{M s}^{-1}$ )	$\text{IC}_{50}^a$ ( $\mu\text{M}$ )	% inhibition at 200 $\mu\text{M}$
JNK2 WT	1.65 $\pm$ 0.1	1 $\pm$ 0.15	0.6	2.9 $\pm$ 0.17	70
JNK2 (R127A)	23.6 $\pm$ 1.1	1.4 $\pm$ 0.3	0.06	14 $\pm$ 2.1	80
JNK2 (Y130A)	1.87 $\pm$ 0.3	1 $\pm$ 0.04	0.53	2.3 $\pm$ 0.16	95
JNK2 (C163A)	1.33 $\pm$ 0.4	1 $\pm$ 0.065	0.75	37 $\pm$ 2.5	37
JNK2 (T164A)	0.73 $\pm$ 0.18	1.1 $\pm$ 0.064	1.5	13.6 $\pm$ 1.5	39
JNK2 (W324A)	2.3 $\pm$ 0.15	1.06 $\pm$ 0.075	0.46	16.6 $\pm$ 0.17	98
JNK2 (D326A)	2 $\pm$ 0.83	0.8 $\pm$ 0.08	0.4	2.8 $\pm$ 0.32	71

<sup>a</sup> $\text{IC}_{50}$  determined as described in Methods section. Data were fitted to eq 4. <sup>b</sup>Initial velocity data at different concentrations of c-Jun were fitted to eq 1.

the kinase binding ATP and phosphorylating itself. When the cells were treated with SP600125,<sup>44</sup> an inhibitor of JNK that binds within the ATP binding pocket of JNK2 $\alpha$ 2, its autophosphorylation was inhibited. However, when the cells were stimulated using anisomycin, SP600125 was no longer able to inhibit JNK2 $\alpha$ 2 phosphorylation, presumably because it was mediated by the activated MKK4 and MKK7 kinases (Figure 3c). These observations are consistent with the proposed mechanisms of each inhibitor. Whereas (–)-zuonin A inhibits the binding of JNK2 $\alpha$ 2 to the upstream kinases and downstream substrates, it fails to prevent JNK2 from phosphorylating itself. In contrast, SP600125 prevents both JNK2 $\alpha$ 2 autophosphorylation and substrate phosphorylation but does not inhibit the ability of MKK4 and MKK7 to phosphorylate JNK2 $\alpha$ 2.

As noted above, (–)-zuonin A also impedes the phosphorylation of JNKs in cells following stimulation by anisomycin (Figure 1c). While the ability of (–)-zuonin A to inhibit JNK phosphorylation in HEK293 cells might stem from its ability to impede the docking of MKK4 and MKK7 to JNK, it is also possible that other JNK-protein interactions are important. It is notable that the  $\text{ED}_{50}$  for inhibiting JNK phosphorylation is around 25  $\mu\text{M}$ , roughly 1 order of magnitude higher than the  $\text{IC}_{50}$  value obtained in the kinase assays. Bioavailability may decrease the cellular potency of (–)-zuonin A compared to the *in vitro* kinase assay. It should be noted that the typical  $\text{ED}_{50}$  for an ATP-competitive kinase inhibitor is in the micromolar range, reflecting the high concentration of competing MgATP in cells. For example SP600125 is an ATP-competitive inhibitor of JNK with an *in vitro* cell-free  $\text{IC}_{50}$  of ~40–100 nM, while its  $\text{ED}_{50}$  for JNK activity in Jurkat T cells is ~10  $\mu\text{M}$ .<sup>44</sup> In this regard (–)-zuonin A may be regarded as a useful starting point for the development of more potent analogues. We conclude that (–)-zuonin A inhibits JNK by a protein-competitive mechanism where the competing protein is a JNK substrate, an upstream kinase or a scaffold. It remains to be determined how (–)-zuonin A affects the binding of other proteins, such as other substrates or the MAPK-specific phosphatases that dephosphorylate JNKs.

**Inhibition of Akt Activation.** JNK2 $\alpha$ 2 is reported to promote the tumorigenicity of human glioblastoma cells through Akt, whose activation is dependent on the presence of constitutively active JNK2 in U87MG cells.<sup>12,45</sup> Accordingly, we tested the effect of (–)-zuonin A and a DMSO control on Akt activation in HEK293T cells by monitoring Akt phosphorylation at Ser-473.<sup>46</sup> HEK293T cells were transfected with WT-JNK2 $\alpha$ 2 and treated with a DMSO control or different concentrations of (–)-zuonin A without induction by anisomycin. Interestingly, (–)-zuonin A was able to inhibit Akt phosphorylation mediated by JNK2 $\alpha$ 2 (Figure 3d). Thus,

(–)-zuonin A has potential as a modulator of Akt activity resulting from constitutive JNK2 $\alpha$ 2 activity.

**Selectivity of (–)-Zuonin A against Other MAPKs in Cells.** To profile the selectivity of (–)-zuonin A, we examined its ability to inhibit other MAP kinases, including ERK1, ERK2, p38MAPK $\alpha$ , p38MAPK $\beta$ , p38MAPK $\gamma$ , and p38MAPK $\delta$  in kinase assays. (–)-Zuonin A showed little ability to inhibit any of these MAP kinases, supporting the notion that (–)-zuonin A is selective for the JNKs (Table 1). This was further verified in HEK293T cells. For the p38 MAPK pathway, neither the phosphorylation of p38MAPK nor ATF2 (Activating Transcription Factor 2), a transcription factor substrate for the p38 MAPK kinase, was affected after treatment of cells with 100  $\mu\text{M}$  (–)-zuonin A (Figure 3f). Similarly, 100  $\mu\text{M}$  (–)-zuonin A had no effect on the phosphorylation of ERK or its protein substrate p-90RSK (Figure 3e).

**Chemical Genetics: Altering JNK Sensitivity to (–)-Zuonin A. *In Vitro* Studies.** A binding mode for the binding of (–)-zuonin A to JNK was predicted using molecular dynamic simulation (Figure 4a). The benzodioxole groups on (–)-zuonin A can potentially interact with both charged and nonpolar residues on JNK. The modeling suggests that one benzodioxole group may engage in  $\pi$ -stacking interactions with Tyr-130 and Trp-324 of JNK, with the other ring binding in the region of Asp-126, Arg-127, Cys-163, and Thr-164. We were interested in verifying the binding site of (–)-zuonin A and also wanted to identify residues whose mutation might compromise its binding. Accordingly, the following mutations, R127A, Y130A, C163A, T164A, W324A, and D326A, were incorporated individually into JNK2 $\alpha$ 2. Initially, we tested whether any of the mutants exhibited altered kinetic parameters using c-Jun as the protein substrate. Only the R127A mutant of JNK2 $\alpha$ 2 exhibited altered kinetic parameters for c-Jun phosphorylation, with the mutation resulting in an increase in the  $K_m$  for c-Jun of 15-fold (Table 2). As shown in Figure 4b and Table 2, the C163A, R127A, and T164A mutants all exhibited an increased  $\text{IC}_{50}$ , providing some support for the binding model. Interestingly, these mutations all resulted in a 2-fold decrease in the observed level of maximal inhibition at saturating (–)-zuonin A. In contrast, the Y130A and W324A mutants not only retained their ability to bind (–)-zuonin A but also displayed a shift in mechanism from partial to full inhibition (Table 2). Thus, mutation of Tyr-130 or Trp-324 to alanine results in a mutant that phosphorylates c-Jun normally but is significantly more sensitive to (–)-zuonin A than wild type JNK2.

**Cellular Studies.** The C163A and Y130A mutants exhibited similar abilities to phosphorylate c-Jun, yet markedly different sensitivities to (–)-zuonin A, suggesting that they could be used in chemical genetic studies<sup>47</sup> to elucidate the role of JNK2

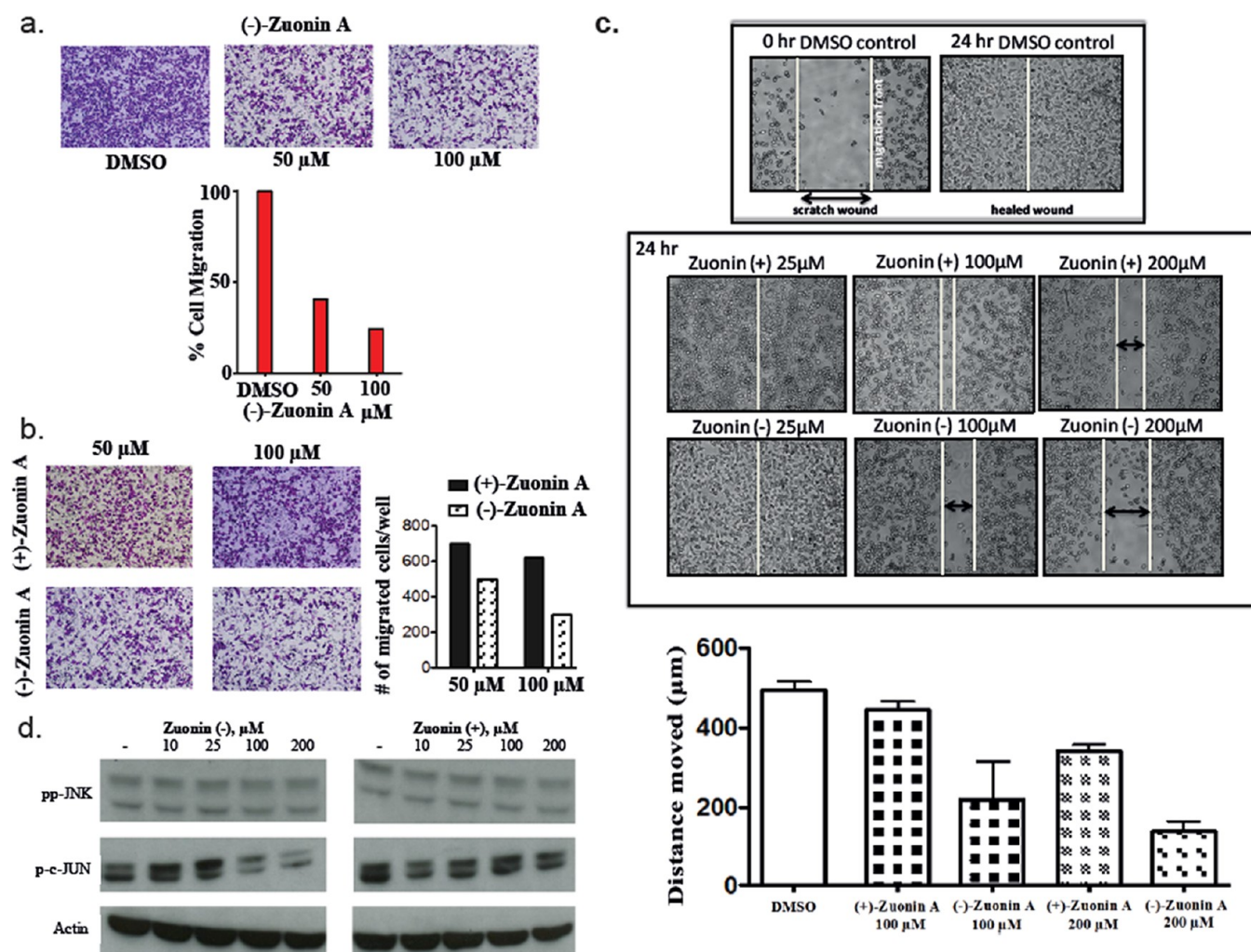


**Figure 5.** (–)-Zuonin A inhibits MDA MB 231 breast cancer cell migration more than (+)-zuonin A. (a) Representative images of migrated cells on the underside of a transwell membrane stained with crystal violet dye. A concentration of 50–100  $\mu\text{M}$  of (–)-zuonin A significantly reduces the number of cells that travel through the transwell pores to successfully reach the underside of the transwell membrane (migrated cells) in comparison to the untreated cells. (b) (–)-Zuonin A inhibits MDA MB 231 breast cancer cell migration more than (+)-zuonin A at 100  $\mu\text{M}$ . This experiment was independently repeated three times. (c) Wound healing assay. After treatment of MDA MB 231 breast cancer cell with different concentrations of (–)-zuonin and (+)-zuonin A, a scratch wound was created in each sample, and culture media were replaced with 1% FBS-containing media. Wound closure was measured at time 0 and at 24 h post-wounding. Graphical analysis representative of three independent experiments. (d) MDA MB 231 cells were treated with a DMSO control or (–)-zuonin A (10–200  $\mu\text{M}$ ) for 12 h before lysing the cells. Lysates were fractionated by SDS-PAGE (10% gel) and subjected to Western blot analysis in order to detect the phosphorylated forms of c-Jun and JNK.

in cells. JNK2 $\alpha$ 2 (C163A) and JNK2 $\alpha$ 2 (Y130A) were transfected into HEK293T cells, which were subsequently treated with varied concentrations of (–)-zuonin A. Autophosphorylation of JNK2 $\alpha$ 2 and the subsequent phosphorylation of c-Jun were examined and compared to cells that were not transfected. The extent of phosphorylation of the JNK2 mutants was similar to exogenously expressed WT JNK2 $\alpha$ 2 in the absence of (–)-zuonin A (compare Figures 3b and 4c). As expected, autophosphorylation of transfected and endogenous JNK was unaffected by (–)-zuonin A treatment (Figure 4c). However, a significant difference in the dose-dependence of c-Jun phosphorylation is evident between cells transfected with JNK2 $\alpha$ 2 (Y130A) and those transfected with JNK2 $\alpha$ 2 (C163A). Cells transfected with JNK2 $\alpha$ 2 Y130A are more sensitive to (–)-zuonin A than either those transfected with WT JNK2 $\alpha$ 2 or those not transfected at all. Strikingly, cells transfected with JNK2 $\alpha$ 2 (C163A) are unresponsive to (–)-zuonin A (Figures 3b and 4c). While further studies are

required to determine whether these mutations affect interactions between JNK and other proteins (e.g., other substrates) they hold promise as chemical-genetic tools to examine the function of JNK2 in cells.

**(–)-Zuonin A Impedes Migration of Breast Cancer Cells.** The invasion-metastatic cascade involves a series of events whereby tumor cells leave the primary tumor, intravasate into the circulation, extravasate at distant tissues, and establish micrometastases that may grow into macroscopic secondary tumors.<sup>48</sup> Cell migration is an early requirement for tumor metastasis, so inhibition of cell migration provides a potential strategy to inhibit metastasis.<sup>49</sup> The JNK pathway is known to play important roles in cell migration (e.g., ref 50), and previously, we demonstrated an ability of a peptide that is selective for JNK2 to inhibit breast cancer cell migration.<sup>16</sup> Therefore, we examined whether (–)-zuonin A or (+)-zuonin A inhibited chemotactic cell migration of a highly metastatic human breast cancer cell line, namely, MDA-MB-231 in a



transwell assay. MDA-MB-231 cells were treated with DMSO, (–)-zuonin A (50  $\mu$ M and 100  $\mu$ M), or (+)-zuonin A (50 and 100  $\mu$ M) (Figure 5) overnight. Cell viability was monitored during the migration assay and found to be unaffected by the addition of the compounds. Untreated MDA-MB-231 cells showed robust migration in response to serum, while cells treated with 50 and 100  $\mu$ M (–)-zuonin A exhibited approximately 45% and 80% inhibition of migration, respectively (Figure 5a). Although (+)-zuonin A was able to mildly suppress cell migration, there is a clear difference between the ability of the two isomers in this respect (Figure 5b), supporting the notion that JNK2 signaling contributes to breast cancer cell migration. Since cells also use their migration machinery during wound closure, a scratch wound closure assay was used to examine the effect of zuonin A on the ability of MDA-MB-231 cells to repair wounds. Wound assays were performed to measure the influence of 25–200  $\mu$ M of (–)-zuonin A and (+)-zuonin A on cell migration to close a scratch wound over time. Cell viability was monitored during the wound assay and found to be unaffected by the addition of the compounds up to 200  $\mu$ M. Both 100 and 200  $\mu$ M (–)-zuonin A was sufficient to inhibit wound closure in MDA MB 231 cells (Figure 5c). Like the chemotaxis-based transwell migration assay, (–)-zuonin A showed notable potency to inhibit wound closure in comparison to (+)-zuonin A. These data are consistent with the observed potency of the two isomers toward JNK in both cell-free (Table 1) and cell-based *in vitro* assays (Figures 1 and 5d). However, the possibility of additional affects of (–)-zuonin A on cell migration, which are not attributable to JNK2, cannot be ruled out.

To summarize, we report the asymmetric synthesis of the lignans (–)-zuonin A and (+)-zuonin A and established the absolute configuration of the natural products. We show that (–)-zuonin A is a selective inhibitor of the JNKs and identify two mechanisms as likely contributors to its ability to inhibit JNK signaling in cells: (–)-zuonin A inhibits (i) JNK activation by MKK4 and MKK7 and (ii) substrate phosphorylation. In both cases it impedes the binding of the corresponding protein to the D-recruitment site of JNK. While (+)-zuonin A binds JNK, it is not an effective inhibitor. The activity of (–)-zuonin toward JNK is the basis for its ability to inhibit Akt signaling and breast cancer cell migration. Mutations in the predicted binding site for (–)-zuonin A can render it significantly more or less sensitive to inhibition than wild type JNK2, allowing for the design of potential chemical genetic experiments. These studies suggest that the biological activity reported for other lignans, such as saucerneol F and zuonin B, may be the result of blocking protein–protein interactions within MAPK cascades. These discoveries hold the potential to introduce future analogues into the arsenal of therapeutics now used to fight cancer cell metastasis.

## METHODS

Cell culture, Western blot analysis, and cell migration assays are described in detail in the Supporting Information.

**Kinase Activity Assay.** MAP kinase assays were conducted as described in the Supporting Information.

**Expression, Purification, and Activation of Tagless MAP Kinases, GST-ATF2 (1-115), GST-C-Jun (1-221), and His-Ets-1 (1-138).** Different MAP kinases and protein substrates were expressed, purified, and then activated (if required) according to the methods described in the Supporting Information.

**Molecular Dynamics Simulations.** Molecular dynamics simulations for (–)-zuonin A bound to JNK are described in the Supporting Information.

**Data Analysis. Steady-State Kinetic Experiments.** Reactions were carried out as mentioned in the kinase activity assay except in the kinetic mechanism study, where we varied concentrations of substrate (c-Jun) and (–)-zuonin A. Initial rates were determined by linear least-squares fitting to plots of product against time. Reciprocal plots of  $1/v$  against  $1/s$  were checked for linearity, before the data were fitted to eq 1 using a nonlinear least-squares approach, assuming equal variance for velocities, using the program Kaleidagraph 3.5 (Synergy software). Values for kinetic constants were then obtained using the program Sigma plot by fitting the kinetic data to the relevant overall equation. Data conforming to linear competitive inhibition were fitted to eq 2; data conforming to hyperbolic mixed inhibition were fitted to eq 3, which corresponds to an equation for partial competitive inhibition. Dose–response curves for data conforming to inhibition were fitted to eq 4.

$$\frac{V_0}{V_{\max}^{\text{app}}} = \frac{s}{K_{\text{mS}}^{\text{app}} + s} \quad (1)$$

$$\frac{V_0}{V_{\max}^{\text{app}}} = \frac{s}{K_{\text{mS}}^{\text{app}}(1 + i/K_{\text{ic}}^{\text{app}}) + s} \quad (2)$$

$$\frac{V_0}{V_{\max}^{\text{app}}} = \frac{s}{K_{\text{mS}}^{\text{app}} \left( \frac{1 + \frac{i}{K_{\text{i}}^{\text{app}}}}{1 + \frac{\beta i}{\alpha K_{\text{i}}^{\text{app}}}} \right) + s \left( \frac{1 + \frac{i}{\alpha K_{\text{i}}^{\text{app}}}}{1 + \frac{\beta i}{\alpha K_{\text{i}}^{\text{app}}}} \right)} \quad (3)$$

$$V_0 = V_{00} - \left( V_{00} \frac{i}{i + (K_{50})} \right) + V' \quad (4)$$

The parameters used in deriving equations are defined as follows;  $V_0$ , observed rate;  $V_{\max}^{\text{app}}$ , apparent maximum rate;  $s$ , concentration of substrate S;  $K_{\text{mS}}^{\text{app}}$ , apparent Michaelis constant for substrate S;  $i$ , concentration of inhibitor I;  $K_{\text{i}}^{\text{app}}$  or  $K_{\text{ic}}^{\text{app}}$ , apparent competitive inhibition constant for inhibitor I;  $\alpha K_{\text{i}}^{\text{app}}$ , apparent uncompetitive inhibition constant for inhibitor I;  $\beta V_{\max}^{\text{app}}$ , apparent maximum rate for enzyme inhibitor complex;  $V_{00}$ , observed rate in the absence of inhibitor,  $V'$ , observed rate at saturating inhibitor I or activator x,  $K_{50}$ , concentration that leads to half the maximal change in  $V_0$ .

## ASSOCIATED CONTENT

### Supporting Information

This material is available free of charge via the Internet at <http://pubs.acs.org>.

## AUTHOR INFORMATION

### Corresponding Author

\*E-mail: [kinases@me.com](mailto:kinases@me.com).

### Notes

The authors declare no competing financial interest.

## ACKNOWLEDGMENTS

Financial support was from grants from the National Institute of General Medical Sciences (R01GM059802), the Welch Foundation (F-1390), and Texas Institute for Drug & Diagnostic Development (H-F-0032) to K.N.D. Financial support for the computational studies was from the National Institute of General Medical Sciences (R01GM079686) to P.R. The authors gratefully acknowledge supercomputer time provided by the Texas Advanced Computing Center (TACC) and TeraGrid (MCB100057) at the University of Texas at Austin. T.S.K. acknowledges The University of Texas at Austin for The A.D. Hutchinson Student Endowment Fellowship. J.H.

is grateful to Duke University for funding this work, to the North Carolina Biotechnology Center (NCBC) (Grant No. 2008-IDG-1010) for funding of NMR instrumentation, and to the National Science Foundation (NSF) MRI Program (Award ID No. 0923097) for funding mass spectrometry instrumentation. The authors thank G. Mills for providing the cell lines and reagents for the migration assays and providing laboratory space and advice to S.M., E. Anslyn for providing laboratory space and advice to J.J., P. LoGrasso for providing JNK plasmids, and A. Syrett for preparing the TOC figure. The content is solely the responsibility of the authors and does not necessarily represent the official views of the National Institute of General Medical Sciences or the National Institutes of Health.

## REFERENCES

- (1) Gupta, S., Barrett, T., Whitmarsh, A. J., Cavanagh, J., Sluss, H. K., Derijard, B., and Davis, R. J. (1996) Selective interaction of JNK protein kinase isoforms with transcription factors. *EMBO J.* 15, 2760–2770.
- (2) Davis, R. J. (2000) Signal transduction by the JNK group of MAP kinases. *Cell* 103, 239–252.
- (3) Bogoyevitch, M. A., Ngoei, K. R., Zhao, T. T., Yeap, Y. Y., and Ng, D. C. (1804) c-Jun N-terminal kinase (JNK) signaling: recent advances and challenges. *Biochim. Biophys. Acta*, 463–475.
- (4) Manning, A. M., and Davis, R. J. (2003) Targeting JNK for therapeutic benefit: from junk to gold? *Nat. Rev. Drug Discovery* 2, 554–565.
- (5) Huang, P., Han, J., and Hui, L. (2010) MAPK signaling in inflammation-associated cancer development. *Protein Cell* 1, 218–226.
- (6) Chen, F., and Castranova, V. (2009) Beyond apoptosis of JNK1 in liver cancer. *Cell Cycle* 8, 1145–1147.
- (7) Sancho, R., Nateri, A. S., de Vinuesa, A. G., Aguilera, C., Nye, E., Spencer-Dene, B., and Behrens, A. (2009) JNK signalling modulates intestinal homeostasis and tumourigenesis in mice. *EMBO J.* 28, 1843–1854.
- (8) Vivanco, I., Palaskas, N., Tran, C., Finn, S. P., Getz, G., Kennedy, N. J., Jiao, J., Rose, J., Xie, W., Loda, M., Golub, T., Mellingerhoff, I. K., Davis, R. J., Wu, H., and Sawyers, C. L. (2007) Identification of the JNK signaling pathway as a functional target of the tumor suppressor PTEN. *Cancer Cell* 11, 555–569.
- (9) She, Q. B., Chen, N., Bode, A. M., Flavell, R. A., and Dong, Z. (2002) Deficiency of c-Jun-NH(2)-terminal kinase-1 in mice enhances skin tumor development by 12-O-tetradecanoylphorbol-13-acetate. *Cancer Res.* 62, 1343–1348.
- (10) Tong, C., Yin, Z., Song, Z., Dockendorff, A., Huang, C., Mariadason, J., Flavell, R. A., Davis, R. J., Augenlicht, L. H., and Yang, W. (2007) c-Jun NH2-terminal kinase 1 plays a critical role in intestinal homeostasis and tumor suppression. *Am. J. Pathol.* 171, 297–303.
- (11) Tsuki, H., Tnani, M., Okamoto, I., Kenyon, L. C., Emllet, D. R., Holgado-Madruga, M., Lanham, I. S., Joynes, C. J., Vo, K. T., and Wong, A. J. (2003) Constitutively active forms of c-Jun NH2-terminal kinase are expressed in primary glial tumors. *Cancer Res.* 63, 250–255.
- (12) Antonyak, M. A., Kenyon, L. C., Godwin, A. K., James, D. C., Emllet, D. R., Okamoto, I., Tnani, M., Holgado-Madruga, M., Moscatello, D. K., and Wong, A. J. (2002) Elevated JNK activation contributes to the pathogenesis of human brain tumors. *Oncogene* 21, 5038–5046.
- (13) Weston, C. R., and Davis, R. J. (2007) The JNK signal transduction pathway. *Curr. Opin. Cell Biol.* 19, 142–149.
- (14) Mitra, S., Lee, J. S., Cantrell, M., and Van den Berg, C. L. (2011) c-Jun N-terminal kinase 2 (JNK2) enhances cell migration through epidermal growth factor substrate 8 (EPS8). *J. Biol. Chem.* 286, 15287–15297.
- (15) Ridley, A. J., Schwartz, M. A., Burridge, K., Firtel, R. A., Ginsberg, M. H., Borisy, G., Parsons, J. T., and Horwitz, A. R. (2003) Cell migration: integrating signals from front to back. *Science* 302, 1704–1709.
- (16) Kaoud, T. S., Mitra, S., Lee, S., Taliaferro, J., Cantrell, M., Linse, K. D., Van Den Berg, C. L., and Dalby, K. N. (2011) Development of JNK2-selective peptide inhibitors that inhibit breast cancer cell migration. *ACS Chem. Biol.* 6, 658–666.
- (17) Zhang, T., Inesta-Vaquera, F., Niepel, M., Zhang, J., Ficarro, S. B., Machleidt, T., Xie, T., Marto, J. A., Kim, N., Sim, T., Laughlin, J. D., Park, H., LoGrasso, P. V., Patricelli, M., Nomanbhoy, T. K., Sorger, P. K., Alessi, D. R., and Gray, N. S. (2012) Discovery of potent and selective covalent inhibitors of JNK. *Chem. Biol.* 19, 140–154.
- (18) Fleming, Y., Armstrong, C. G., Morrice, N., Paterson, A., Goedert, M., and Cohen, P. (2000) Synergistic activation of stress-activated protein kinase 1/c-Jun N-terminal kinase (SAPK1/JNK) isoforms by mitogen-activated protein kinase kinase 4 (MKK4) and MKK7. *Biochem. J.* 352 (Pt 1), 145–154.
- (19) Nitta, R. T., Chu, A. H., and Wong, A. J. (2008) Constitutive activity of JNK2 alpha2 is dependent on a unique mechanism of MAPK activation. *J. Biol. Chem.* 283, 34935–34945.
- (20) Yasuda, J., Whitmarsh, A. J., Cavanagh, J., Sharma, M., and Davis, R. J. (1999) The JIP group of mitogen-activated protein kinase scaffold proteins. *Mol. Cell Biol.* 19, 7245–7254.
- (21) Zhan, X., Kaoud, T. S., Dalby, K. N., and Gurevich, V. V. (2011) Nonvisual arrestins function as simple scaffolds assembling the MKK4-JNK3alpha2 signaling complex. *Biochemistry* 50, 10520–10529.
- (22) Schnieders, M. J., Kaoud, T. S., Yan, C., Dalby, K. N., and Ren, P. (2012) Computational insights for the discovery of non-ATP competitive inhibitors of MAP kinases. *Curr. Pharm. Des.* 18, 1173–1185.
- (23) Stebbins, J. L., De, S. K., Machleidt, T., Becattini, B., Vazquez, J., Kuntzen, C., Chen, L. H., Cellitti, J. F., Riel-Mehan, M., Emdadi, A., Solinas, G., Karin, M., and Pellecchia, M. (2008) Identification of a new JNK inhibitor targeting the JNK-JIP interaction site. *Proc. Natl. Acad. Sci. U.S.A.* 105, 16809–16813.
- (24) Chambers, J. W., Cherry, L., Laughlin, J. D., Figuera-Losada, M., and LoGrasso, P. V. (2011) Selective inhibition of mitochondrial JNK signaling achieved using peptide mimicry of the Sab Kinase Interacting Motif-1 (KIM1). *ACS Chem. Biol.* 6, 808–818.
- (25) Johnson, L. N. (2009) Protein kinase inhibitors: Contributions from structure to clinical compounds. *Q. Rev. Biophys.* 42, 1–40.
- (26) Kaoud, T. S., Yan, C., Mitra, S., Tseng, C.-C., Jose, J., Taliaferro, J. M., Tuohetahuntala, M., Devkota, A., Sammons, R., Park, J., Park, H., Shi, Y., Hong, J., Ren, P., and Dalby, K. N. (2012) From in silico discovery to intracellular activity: targeting the JNK–protein interactions with small molecules, *ACS Medicinal Chemistry Letters*, In press.
- (27) Urzua, A., Freyer, A. J., and Shamma, M. (1987) 2,5-Diaryl-3,4-dimethyltetrahydrofuranoid lignans. *Phytochemistry* 26, 1509–1511.
- (28) Rao, K. V., and Rao, N. S. (1990) Chemistry of Saururus cernuus, VI: Three new neolignans. *J. Nat. Prod.* 53, 212–215.
- (29) Tyagi, O. D., Jensen, S., Boll, P. M., Sharma, N. K., Bisht, K. S., and Parmar, V. S. (1993) Lignans and neolignans from Piper schmidtii. *Phytochemistry* 32, 445–448.
- (30) Kuo, Y.-H., Chen, C.-H., and Lin, Y.-L. (2002) New lignans from the heartwood of *Chamaecyparis obtusa* var. *formosana*. *Chem. Pharm. Bull.* 50, 978–980.
- (31) Konishi, T., Konoshima, T., Daikonya, A., and Kitanaka, S. (2005) Neolignans from Piper futokadsura and their inhibition of nitric oxide production. *Chem. Pharm. Bull. (Tokyo)* 53, 121–124.
- (32) Lu, Y., Suh, S. J., Kwak, C. H., Kwon, K. M., Seo, C. S., Li, Y., Jin, Y., Li, X., Hwang, S. L., Kwon, O., Chang, Y. C., Park, Y. G., Park, S. S., Son, J. K., Kim, C. H., and Chang, H. W. (2012) Sauerneel F, a new lignan, inhibits iNOS expression via MAPKs, NF-kappaB and AP-1 inactivation in LPS-induced RAW264.7 cells. *Int. Immunopharmacol.* 12, 175–181.
- (33) Lee, M. Y., Yuk, J. E., Kwon, O. K., Oh, S. R., Lee, H. K., and Ahn, K. S. (2012) Zuonin B inhibits lipopolysaccharide-induced inflammation via downregulation of the ERK1/2 and JNK pathways in

RAW264.7 macrophages. *Evid. Based Complement. Alternat. Med.*, No. 2012:728196.

(34) Kim, H., Wooten, C. M., Park, Y., and Hong, J. (2007) Stereoselective synthesis of tetrahydrofuran lignans via  $\text{BF}_3 \cdot \text{OEt}_2$ -promoted reductive deoxygenation/epimerization of cyclic hemiketal: synthesis of (-)-odoratisol C, (-)-futokadsurin A, (-)-veraguensin, (+)-fragransin A<sub>2</sub>, (+)-galbelgin, and (+)-talaumidin. *Org. Lett.* 9, 3965–3968.

(35) Kim, H., Kasper, A. C., Moon, E. J., Park, Y., Wooten, C. M., Dewhirst, M. W., and Hong, J. (2009) Nucleophilic addition of organozinc reagents to 2-sulfonyl cyclic ethers: stereoselective synthesis of manassantins A and B. *Org. Lett.* 11, 89–92.

(36) Evans, D. A., Bartroli, J., and Shih, T. L. J. (1981) Enantioselective aldol condensations. 2. Erythro-selective chiral aldol condensations via boron enolates. *J. Am. Chem. Soc.* 103, 2127–2129.

(37) Schreiber, J., Maag, H., Hashimoto, N., and Eschenmoser, A. (1971) Dimethyl(methylene)ammonium iodide. *Angew. Chem., Int. Ed. Engl.* 10, 330–331.

(38) Mandal, M., Yun, H., Dudley, G. B., Lin, S., Tan, D. S., and Danishefsky, S. J. (2005) Total synthesis of guanacastepene a: a route to enantiomeric control. *J. Org. Chem.* 70, 10619–10637.

(39) Abramczyk, O., Rainey, M. A., Barnes, R., Martin, L., and Dalby, K. N. (2007) Expanding the repertoire of an ERK2 recruitment site: cysteine footprinting identifies the D-recruitment site as a mediator of Ets-1 binding. *Biochemistry* 46, 9174–9186.

(40) Niu, L., Chang, K. C., Wilson, S., Tran, P., Zuo, F., and Swinney, D. C. (2007) Kinetic characterization of human JNK2 $\alpha$ 2 reaction mechanism using substrate competitive inhibitors. *Biochemistry* 46, 4775–4784.

(41) Bardwell, A. J., Frankson, E., and Bardwell, L. (2009) Selectivity of docking sites in MAPK kinases. *J. Biol. Chem.* 284, 13165–13173.

(42) Repici, M., Mare, L., Colombo, A., Ploia, C., Scip, A., Bonny, C., Nicod, P., Salmona, M., and Borsello, T. (2009) c-Jun N-terminal kinase binding domain-dependent phosphorylation of mitogen-activated protein kinase kinase 4 and mitogen-activated protein kinase kinase 7 and balancing cross-talk between c-Jun N-terminal kinase and extracellular signal-regulated kinase pathways in cortical neurons. *Neuroscience* 159, 94–103.

(43) Clerk, A., and Sugden, P. H. (1997) Cell stress-induced phosphorylation of ATF2 and c-Jun transcription factors in rat ventricular myocytes. *Biochem. J.* 325 (Pt 3), 801–810.

(44) Bennett, B. L., Sasaki, D. T., Murray, B. W., O'Leary, E. C., Sakata, S. T., Xu, W., Leisten, J. C., Motiwala, A., Pierce, S., Satoh, Y., Bhagwat, S. S., Manning, A. M., and Anderson, D. W. (2001) SP600125, an anthrapyrazolone inhibitor of Jun N-terminal kinase. *Proc. Natl. Acad. Sci. U.S.A.* 98, 13681–13686.

(45) Cui, J., Han, S. Y., Wang, C., Su, W., Harshyne, L., Holgado-Madruga, M., and Wong, A. J. (2006) c-Jun NH(2)-terminal kinase 2 $\alpha$ 2 promotes the tumorigenicity of human glioblastoma cells. *Cancer Res.* 66, 10024–10031.

(46) Alessi, D. R., Andjelkovic, M., Caudwell, B., Cron, P., Morrice, N., Cohen, P., and Hemmings, B. A. (1996) Mechanism of activation of protein kinase B by insulin and IGF-1. *EMBO J.* 15, 6541–6551.

(47) Kawasumi, M., and Nghiem, P. (2007) Chemical genetics: elucidating biological systems with small-molecule compounds. *J. Invest. Dermatol.* 127, 1577–1584.

(48) Bacac, M., and Stamenkovic, I. (2008) Metastatic cancer cell. *Annu. Rev. Pathol.* 3, 221–247.

(49) Valastyan, S., Reinhardt, F., Benaich, N., Calogrias, D., Szasz, A. M., Wang, Z. C., Brock, J. E., Richardson, A. L., and Weinberg, R. A. (2009) A pleiotropically acting microRNA, miR-31, inhibits breast cancer metastasis. *Cell* 137, 1032–1046.

(50) Huang, C., Jacobson, K., and Schaller, M. D. (2004) A role for JNK-paxillin signaling in cell migration. *Cell Cycle* 3, 4–6.

(51) Heo, J. S., Kim, S. K., Seo, C. I., Kim, Y. K., Sung, B. J., Lee, H. S., Lee, J. I., Park, S. Y., Kim, J. H., Hwang, K. Y., Hyun, Y. L., Jeon, Y. H., Ro, S., Cho, J. M., Lee, T. G., and Yang, C. H. (2004) Structural basis for the selective inhibition of JNK1 by the scaffolding protein JIP1 and SP600125. *EMBO J.* 23, 2185–2195.